

GROWTH STAGES AND BIOMASS MODEL OF KALIDIUM: A CASE STUDY OF THE HEIHE RIVER BASIN NORTHWEST CHINA

PANG, W. L.^{1,2} – PANG, W. J.^{3,4,5*} – GUO, K.⁶ – QI, W. Q.^{1,2} – GAO, T. S.^{1,2} – XU, M. Q.^{1,2}

¹Xining Integrated Natural Resources Survey Centre, China Geological Survey (CGS), Xining 810099, China

²Observation Station of Subalpine Ecology Systems in the Middle Qilian Mountains, Zhangye, Gansu 734000, China

³Northwest Institute of Eco-Environment and Resources, CAS, Lanzhou 730070, China

⁴Key Laboratory of Petroleum Resources, Gansu Province, Lanzhou 730000, China

⁵University of Chinese Academy of Sciences, Beijing 100049, China

⁶Qinghai Branch of China Petroleum Engineering Construction Co., LTD, Dunhuang 736202, China

*Corresponding author
e-mail: 15101212030@163.com

(Received 17th Apr 2024; accepted 2nd Sep 2024)

Abstract. The desert ecosystem, with its delicate balance, plays a pivotal role in terrestrial environments, providing crucial ecological services such as windbreak, sand fixation, and soil enhancement. In the arid expanses of the Heihe River Basin in western China, the desert landscape accounts for approximately 76.94% of the region's total area. Among the diverse desert flora, the *Kalidium* shrub stands as a prominent representative, warranting an in-depth investigation into its growth processes and biomass dynamics. This case study delves into the morphological parameters of *Kalidium*'s canopy and root systems, identifying distinct growth stages through a fractal statistical model. By applying modified Malthusian equations, we explore the relationships between crown width/branch height and ground diameter/root length, discussing the morphological implications of the γ value on relative growth rates. Our findings reveal a growth pattern for the canopy that transitions from a flattening-vertical to a near-hemispherical shape, while the root system exhibits a vertical-horizontal to near-cone trend. We deduce a generalized allometric fractal model for estimating the canopy and root biomass, optimizing the use of easily measurable parameters such as branch height (H) and canopy area (SA) through correlation analysis. This study successfully establishes a well-fitting, non-destructive biomass estimation model for *Kalidium* scrubs, providing a foundation for future ecological assessments and management strategies in desert ecosystems.

Keyword: desert, fractal statistical model, allometric fractal model, biomass

Introduction

Deserts, encompassing about 20% of the Earth's land area, are critical components of terrestrial ecosystems, with their biomass and productivity serving as key indicators of their fundamental characteristics (Houghton et al., 2009). These indicators are essential for studying material cycles, energy flows, and assessing the productive potential of desert environments, thus informing their management (Cai et al., 2009). Biomass research has long been a focal point in ecology, as it underpins the study of material and energy exchanges within ecosystems and is a vital measure for evaluating the strength

of ecological communities or the functionality of ecological systems (Zheng and Shang, 2007; Lu and Gong, 2009; Wang and He, 2017).

Shrubs are integral to desert ecosystems, playing a significant role in their conservation, restoration, and reconstruction (Zheng and Shang, 2007). Research on shrub biomass is paramount for the preservation and rehabilitation of desert ecosystems, offering insights into material and energy flows, natural regeneration, and systematic nutrient accumulation (Lu and Gong, 2009). In Chinese desert regions, shrub lands cover vast areas, yet they have received less attention compared to forest ecosystems, partly due to their relatively lower biomass and density levels (Houghton et al., 2009; Dong et al., 2024). Traditional methods for studying shrub biomass, such as direct harvest, are inherently destructive, posing challenges for long-term studies with identical samples and requiring extensive fieldwork and sample processing. Consequently, there is a growing interest in non-destructive methods for measuring shrub biomass, leveraging the close relationship between above-ground biomass and easily measurable growth indicators.

The genus "*Kalidium*", a member of the Amaranthaceae family, is a perennial woody shrub commonly found in deserts, noted for its salt tolerance. Despite its lower transpiration intensity compared to typical psammophytes, *Kalidium* maintains relatively high biomass and above-ground residue during winter, providing benefits for winter grazing and livestock feeding in arid regions (Ren, 2008). It also plays a vital role in preventing sand erosion, stabilizing sand, reducing soil salinity, and increasing soil organic matter (Zhao et al., 2002). Given the fragility of desert ecosystems, non-damaging modeling methods are preferred for studying the biomass of "*Kalidium*". Allometry, a fundamental biological principle, reveals the disparities between various components or subsystems within an organism or group of organisms through their morphological structure and physiological functionality (Zeng, 2015; Tao and Zhang, 2013). The allometric growth model aligns with plant growth patterns and development trends, offering a mechanistic approach to accurately reflect changes in shrub biomass concerning plant morphology (Enquist et al., 1999; Niklas, 2004; Wang et al., 2012; Huang and Di, 2011).

The Fractal Theory, introduced by Mandelbrot in the 1970s, provides a quantitative framework for understanding complex, orderly geometric phenomena in nature that traditional Euclidean geometry cannot capture (Mandelbrot, 1982). It has become a powerful tool for analyzing complex issues in ecology, primarily applied to analyze fractal dimensions and study the characteristics of objects and spatial patterns in the natural world (Chang et al., 1996). Currently, Fractal Theory finds wide applications in various areas of plant research such as forestry (Gao et al., 2004), grassland science (Li and Ling, 2011), plant morphological simulation (Chang and Wu, 1996), and population spatial patterns (Zhang et al., 2012). In the context of this study, the Fractal Theory and allometric principles are employed to investigate the fractal characteristics of *Kalidium*, delineate its growth stages, simulate its growth processes, and derive a biomass estimation model. This research aims to fill the knowledge gap regarding the biomass of *Kalidium* shrub in the Heihe River Basin by providing a scientific basis for non-destructive and timely evaluation of its biomass.

Materials and methods

Study area

The study area is situated within the Heihe River Basin, at the core of the Hexi Corridor in China (*Fig. 1*). The geographical coordinates span from 98° to 101°30' East

longitude and 38° to 42° North latitude. This region is defined by its arid climate, with precipitation that is infrequent and tends to be concentrated, a landscape shaped by prevalent winds, an abundance of sunshine, intense solar radiation, and pronounced daily temperature fluctuations.

The desert ecosystem, located in the middle and lower reaches of the study area, witnesses a gradual decrease in precipitation from 250 mm in the eastern part to below 50 mm towards the western fringes. Concurrently, evaporation rates escalate from less than 2000 mm in the east to a staggering 4000 mm plus in the west. The area is rich in solar and thermal energy resources, with an average annual temperature hovering between 2.8 and 7.6°C, and the duration of daylight ranging from 3000 to 4000 h. Progressing further downstream to the Delta Oasis, in the inland hinterland continental climate is characteristic. This is typified by sparse rainfall, vigorous evaporation, substantial temperature variations, robust winds, and a significant presence of sand. The average annual precipitation is a 42 mm, while the evaporation intensity reaches an average of 3755 mm. The annual temperature averages 8.0°C, with values of 41.8°C the highest and -35.3°C the lowest. The sunshine duration each year falls between 3325.6 and 3432.4 h, with relative humidity levels between 32 to 35%. The average annual wind speed is 4.2 m/s, with gusts reaching a peak of 15.0 m/s.

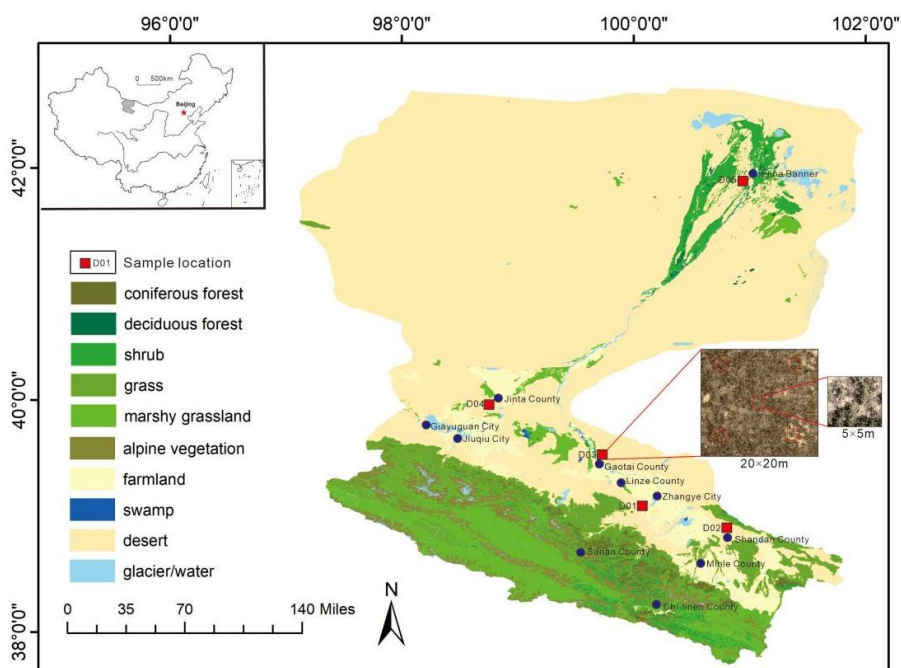


Figure 1. Location map of the study area

The vegetation in the middle and lower reaches of the study area is predominantly composed of temperate shrubs and semi-shrubs typical of desert biomes. In the lower reaches, particularly within the depressions on either side of the delta and around the edges of alluvial fans, one can find thriving desert vegetation, including riparian forests, shrubs, and meadow flora. Notable arboreal species include *Populus euphratica*, *Tamarix ramosissima*, *Kalidium*, and *Haloxylon ammodendron*. The plant species in these desert ecosystems do not significantly deviate from those found in the middle reaches, thereby showcasing a quintessential natural desert oasis landscape.

Field survey

Between July and August 2020, five plots were selected across the study area, representing a range of similar environmental conditions, robust vegetation, intact community structures, and minimal human interference. Within each plot, a grid of five quadrats, each measuring 20 m by 20 m, was established. Additionally, five smaller quadrats, each 1 meter by 1 meter, were positioned in the inner corner and center of each larger quadrat, resulting in a total of 25 small quadrats and 234 *Kalidium* shrub clumps. This stratified sampling technique ensured comprehensive, stable, and precise data on desert shrublands, particularly considering the maximum annual bioaccumulation.

Measurement of shrub morphological attributes

A variety of morphological attributes, including branch height (H), crown dimensions (a , b), ground diameter (GD), and root length (R), were measured on *Kalidium* shrubs within the designated quadrats. Branch height (H) was determined using a tape measure. Ground diameter (GD) was assessed using calipers at a 120° lateral angle; three measurements were taken, and their average was recorded. Crown width (CW) was ascertained by measuring the maximum and minimum diameters in vertical cross-sections (a , b), with the average value representing CW . Further calculations were performed to derive the crown area (CA) and crown volume (CV). Root length (R) was measured in its entirety using a tape measure after complete excavation.

Biomass quantification of shrubs

Within the $1\text{ m} \times 1\text{ m}$ quadrats, above-ground biomass (WA) samples were collected by severing the shrub at ground level. The withered leaves and current year's branches were separated and their fresh weight was measured. The samples were then transported to the laboratory, dried in an oven at 85°C until a constant weight was achieved, and then re-weighed using a balance accurate to 0.01 g.

Fractal statistical models

Shen Wei (Shen and Zhao, 1998) delivered a thorough exposition of the mathematical foundations of fractal statistical models and introduced an innovative method for estimating fractal dimensions through parameter estimation in nonlinear regression models. To highlight the practical implications of these dimensions, they conducted computer-based simulation studies on fractal statistical models. The fractal statistical model is articulated as follows:

$$N(r) = Cr^{\pm D} \quad r > 0 \quad (\text{Eq.1})$$

In the formula, r symbolizes the characteristic scale, $C > 0$ is known as the scaling constant, and $D > 0$ represents the fractal dimension. $N(r)$ denotes either the count of objects with scales greater than or equal to r (indicated as $N(\geq r)$ with a negative sign before D) or the count of objects with scales less than or equal to r (indicated as $N(\leq r)$ with a positive sign before D). A hallmark of fractal distribution in natural phenomena is the power-law relationship between the count of objects larger or smaller than a specific scale and their respective sizes, thereby exhibiting properties of scale invariance.

Let us designate the research data as $\{x_i\}$, where $I = 1, 2, \dots, N$.

$$N(r) = \sum_{x_i \geq r}^N x_i \quad (\text{Eq.2})$$

By doing so, we derive a dataset $\{N(r_i), r_i\}$. When we substitute these data into *Equation 1* and take the logarithm of both sides, it transforms into a simple linear regression model:

$$\lg N(r) = D \lg r + \lg C \quad (\text{Eq.3})$$

The estimation of the fractal dimension D is achieved using the least squares method. In instances where the scatter plot roughly adheres to two linear segments, suggesting a division of data into two groups, a piecewise fitting approach can be applied. While some boundary points may have clear definitions, others may not. To enhance the objectivity in determining these boundary points, an optimization method is employed during regression analysis using the least squares method within two intervals. The core concept involves identifying suitable boundary points r_{i0} in a manner that minimizes the total sum of squared residuals $E_i (i = 1, 2)$ between the fitted lines in each interval and the original data points.

$$E = E_1 + E_2 = \sum_{i=1}^{i_0} [\lg N(r_i) + D_1 \lg r_i - \lg C_1]^2 + \sum_{i=i_0+1}^n [\lg N(r_i) + D_2 \lg r_i - \lg C_2]^2 \quad (\text{Eq.4})$$

The boundary point, denoted by r_{i0} , is associated with the respective slopes D_1 and D_2 , which correspond to the fractal dimensions of their respective intervals. To assess the significance of the regression equation, both correlation coefficient tests and analysis of variance tests were conducted for each regression equation. This methodology can be extended to scenarios involving more than three linear segments, thus accommodating situations where data can be divided into three or more groups.

Allometric growth fractal theory

Within a biological growth system, considering the interplay among various elements that influence biological growth, we can characterize it using the following differential equation:

$$\begin{aligned} \frac{dQ}{dt} &= f_i(Q_1, Q_2, \dots, Q_n) \\ Q_i(0) &= Q_{i0}, i = 1, 2, \dots, n \end{aligned} \quad (\text{Eq.5})$$

Here, Q_i signifies a measure of any growth element ($i = 1, 2, \dots, n$; n is the number of elements). When focusing on a single element, *Equation 5* can be streamlined to:

$$\frac{dQ}{dt} = f(Q)$$

By applying the aforementioned equation to depict the growth of elements such as biomass (W) and morphological parameters (X_1, X_2, \dots, X_i), and using Taylor series expansion followed by simplification, we derive:

$$\frac{dW(t)}{dt} = a_0 W(t), \frac{dX_1(t)}{dt} = a_1 X_1(t), \dots, \frac{dX_i(t)}{dt} = a_i X_i(t) \quad (\text{Eq.6})$$

Upon solving *Equation 6*, we arrive at:

$$W(t) = C_0 e^{a_0 t}, X_1(t) = C_1 e^{a_1 t}, \dots, X_i(t) = C_i e^{a_i t}$$

where C_0, C_1, \dots, C_i are arbitrary constants. Eliminating the time factor, we obtain:

$$W = \beta_1 X_1^{\alpha_1}, W = \beta_2 X_2^{\alpha_2}, \dots, W = \beta_i X_i^{\alpha_i} \quad (\text{Eq.7})$$

In *Equation 7*, $\alpha_i = \frac{a_0}{a_i}$ is the allometric growth coefficient, and β is a constant. By multiplying i equations together, we derive the following equation:

$$W = (\beta_1 \beta_2 \dots \beta_i)^{\frac{1}{i}} X_1^{\frac{\alpha_1}{i}} X_2^{\frac{\alpha_2}{i}} \dots X_i^{\frac{\alpha_i}{i}} = C X_1^{D_1} X_2^{D_2} \dots X_i^{D_i} \quad (\text{Eq.8})$$

In *Equation 8*, C is a constant, and D_1, D_2, \dots, D_i represent the generalized fractal dimensions of various morphological parameters concerning biomass. Thus, we have formulated the allometric growth fractal model:

$$W = C \prod_{i=1}^n X_i^{D_i} \quad (\text{Eq.9})$$

Taking the natural logarithm of both sides of *Equation 9*, we get:

$$\ln W = D_1 \ln X_1 + \dots + D_i \ln X_i + \ln C \quad (\text{Eq.10})$$

Equation 8 can be fitted using the standard least squares method to estimate the model parameters, which correspond to the fractal dimensions for each morphological parameter concerning biomass. All data calculations, statistical analyses, and plotting were conducted using Minitab 17.0, Microsoft Office 2020 Excel, and SPSS 22.0 software.

Results and discussion

Kalidium shrub canopy characteristics

Statistical characteristics of kalidium shrub canopy parameters

This study presents the statistical properties of canopy parameters for *Kalidium* shrubs, as outlined in *Table 1*. The parameters include branch height, crown dimensions (length and width), crown area, and above-ground biomass. The branch height within the canopy varies from 5.8 to 40.1 cm, with an average of 14.78 cm, exhibiting minimal standard deviation and coefficient of variation. The crown area spans from 32.2 to 1433.89 cm², with an average of 378.14 cm², and shows the highest variability among the measured parameters. The canopy's moisture content ranges between 50% and 80%, while the above-ground dry weight fluctuates from 0.19 to 82.35 g, with an average of 12.16 g, indicating a moderate degree of variation.

Figure 2a, b, c depict the frequency distribution and normal fitting for branch height, crown area, and above-ground dry weight of *Kalidium* shrubs, respectively. Branch height is found to be normally distributed, while crown area and above-ground dry weight show a distribution close to normal. The limited variation in branch height suggests a uniform distribution, in contrast to the greater variability observed in crown area and biomass, indicating a less uniform distribution. These results suggest that the sampled shrubs are representative of the growth conditions within the desert *Kalidium* shrub canopy.

Table 1. Statistical analysis of parameters of 234 *kalidiums*

Parameter	Minimum value	Maximum value	Mean value	Standard deviation	Coefficient of variation
Branch height / cm	5.8	40.1	14.78	4.2398	0.2772
Crown length / cm	8.1	48.3	24.01	7.3347	0.4795
Crown width / cm	4.1	41.5	18.44	6.6343	0.4337
Crown area / cm ²	32.2	1433.89	378.14	247.4318	16.1751
Above-ground fresh weight / g	2.75	148.78	29.69	23.1632	1.5142
Above-ground dry weight / g	0.19	82.35	12.16	11.9617	0.7820

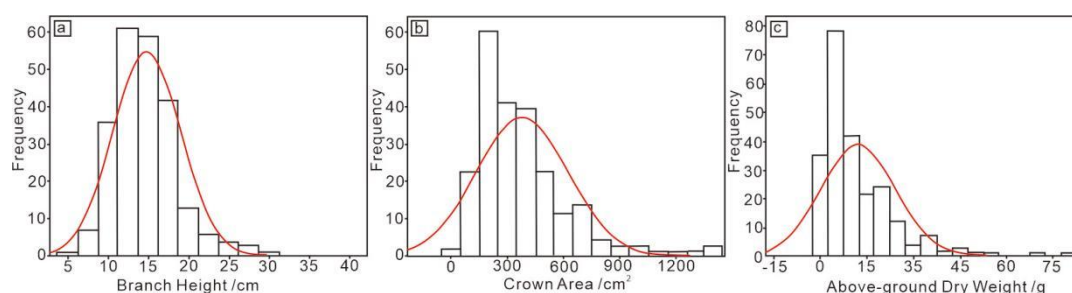


Figure 2. The statistical distribution of branch height, crown width, and above-ground dry weight of *kalidiums*

Fractal characteristics and growth stages of shrub canopy parameters

The application of a fractal statistical model has allowed for the identification of distinct growth stages within the *Kalidium* shrub canopy. The fractal dimensions D highlight characteristic changes at various stages, providing a framework for stage classification.

Figure 3a, b illustrate the distribution of branch height and crown width using a logarithmic transformation, plotted on the $lgr-lgN(r)$ coordinate system. Linear equations, fractal dimensions, and boundary points were derived using the least squares method (Table 2). Notably, the coefficient of determination (R^2) for all models exceeds 0.8, confirming their statistical significance.

Table 2. Fractal model fitting results of canopy branch height and canopy width of *kalidiums*

Morphological parameter	Fractal model	R^2	Fractal dimension	Fitting range
Branch height	$\ln N = -0.1002 \ln r + 2.4443$	0.8230	0.1002	$r \leq 11.82$
	$\ln N = -4.2635 \ln r + 6.9096$	0.9590	4.2635	$11.82 \leq r \leq 26.46$
	$\ln N = -14.882 \ln r + 22.015$	0.9858	14.882	$r \geq 26.46$
Crown area	$\ln N = -0.1611 \ln r + 2.6522$	0.8895	0.1611	$r \leq 308.03$
	$\ln N = -2.5205 \ln r + 8.5238$	0.9713	2.5205	$308.03 \leq r \leq 712.79$
	$\ln N = -3.3271 \ln r + 10.825$	0.9842	3.3272	$r \geq 712.79$

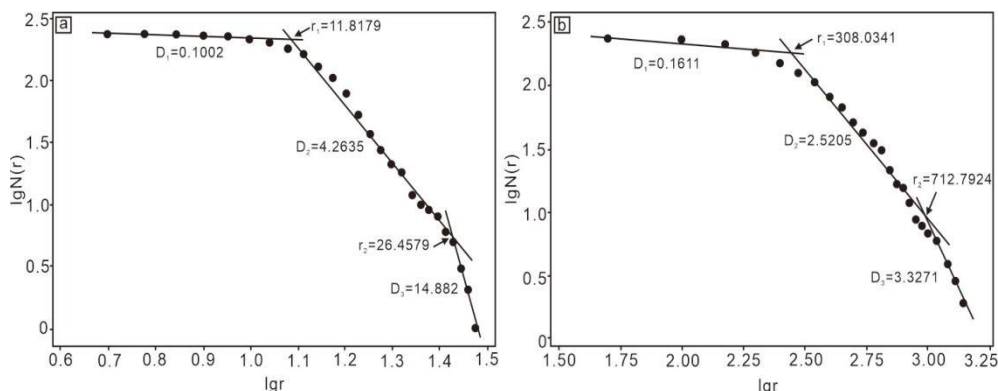


Figure 3. (a) The distribution of branch height $\lg N$ - $\lg r$ of *kalidiums*. (b) The distribution of crown width $\lg N$ - $\lg r$ of *kalidiums*

Desert plants have evolved a suite of distinctive functional traits and growth strategies in response to the long-term challenges posed by extreme environments, which are often defined by scarcity of water, dry conditions, soaring temperatures, and intense solar radiation. These adaptations have endowed them with formidable capabilities for withstanding drought and tolerating various forms of environmental stress (Lortie and Turkington, 2002; Zheng and Shang, 2004). As a result, these plants demonstrate a remarkable plasticity in their morphological characteristics, allowing them to navigate environmental constraints while optimizing their growth rates to the fullest extent possible. This plasticity is a testament to their exceptional adaptability to a wide array of environmental conditions (McConnaughay and Coleman, 1999; Li et al., 2011; Zhang et al., 2016).

In the context of the *Kalidium* shrub community, the fractal distribution characteristics of the crown layer parameters present an opportunity to apply fractal statistical models for the determination of limiting values related to crown morphology (Wang and Wang, 2007). As delineated in section 3.2 by Equation 1, when $N(r)$ equals 1, it signifies that the cumulative number of individuals possessing crown morphological parameters exceeding a certain value r is equivalent to one. Here, $r = C^{1/D}$ represents the threshold limit of crown morphological parameters. Upon calculation, it has been determined that the maximum crown height (H_{max}) is 30.15 cm, and the maximum crown area (CA_{max}) amounts to 1793.42 cm².

By integrating the fractal statistical model with the identified growth intervals and limiting values for shrub height, we have categorized the crown layer samples from the 234 individuals into four distinct growth stages: the Juvenile stage (I), the Growth stage (II), the Mature stage (III), and the Senescent stage (IV), as outlined in Table 3. This classification system provides a comprehensive framework for understanding the developmental trajectory of these desert-adapted shrubs and the dynamic interplay between their morphological plasticity and the harsh environmental conditions they inhabit.

The projection of parameters such as branch height and canopy area for the 234 samples onto a Cartesian coordinate system, as depicted in Figure 4, in tandem with the classification stages detailed in Table 3, greatly simplifies the process of sample categorization. This method allows for a precise differentiation of the various growth stages present within the canopy of *Kalidium* bushes, based on their morphological

characteristics. By leveraging this approach, researchers can efficiently identify and analyze the subtle variations in the developmental stages of these vegetation types, leading to a more nuanced understanding of their ecological dynamics and growth patterns.

Table 3. Criteria for different growth stages of the canopy of *kalidium*s

Growth stage	Juvenile (I)	Growth (II)	Mature (III)	Senescent (IV)
Shrub height / cm	0-11.82	11.82-26.46	26.46-30.15	30.15-0
Crown area / cm ²	0-308.03	308.03-712.79	712.19-1793.42	1793.42-0

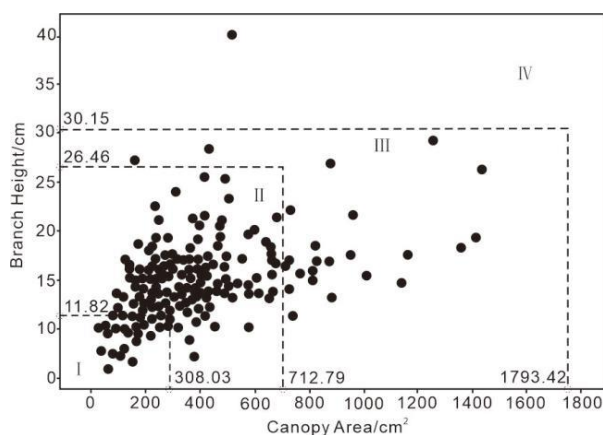


Figure 4. Division of the canopy growth stages of *kalidium*s

Characteristics of *kalidium* shrub root system

Statistical characteristics of *kalidium* shrub canopy parameters

This section presents the statistical characteristics of the *Kalidium* shrub root system, including root length, root diameter, root-to-shoot ratio, and underground biomass parameters. These are detailed in *Table 4*. The root length of the shrubs ranges from 0.8 to 13.1 cm, with an average of 7.28 cm. The standard deviation and coefficient of variation are moderate, indicating a fairly consistent length across the sample. Root diameter varies from 0.2 to 2.1 cm, with an average of 0.8 cm, and shows minimal variation. The root-to-shoot ratio, a key indicator of plant health, ranges from 0.5 to 1.23, with an average of 0.83, suggesting little variability and a stable ratio across the shrubs. The moisture content of the roots is lower, ranging from 20% to 50%, compared to the canopy moisture content. The above-ground dry weight varies significantly, from 0.05 g to a maximum of 23.06 g, with an average of approximately 2.71 g. Despite the high standard deviation, the coefficient of variation remains at a moderate level.

Table 4. Statistical analysis of root parameters in *kalidium* shrubs

Parameter	Minimum value	Maximum value	Average value	Standard deviation	Coefficient of variation
Root length / cm	0.80	13.1	7.28	1.5184	0.0993
Root-to-shoot ratio	0.50	1.23	0.83	0.1719	0.0112
Root diameter / cm	0.20	2.1	0.80	0.4031	0.0264
Underground fresh weight / g	0.16	28.07	3.82	3.6537	0.2389
Underground dry weight / g	0.05	23.06	2.71	2.9462	0.1926

Root length follows a normal distribution, while root diameter and underground dry weight show an approximate normal distribution (Fig. 5). The low variability in root length suggests a homogeneous distribution among individual *Kalidium* shrubs, whereas the higher variability in root diameter and biomass indicates a less uniform distribution. This variability reflects the actual growth status of *Kalidium* shrub roots in the desert.

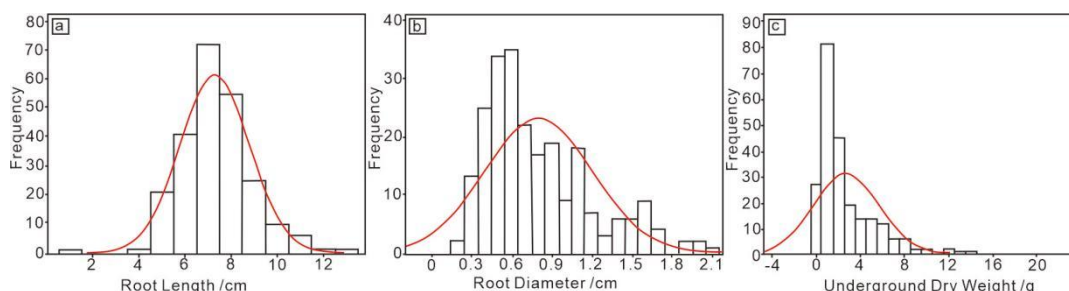


Figure 5. Statistical distribution of root length, ground diameter, and underground dry weight of *Kalidium*

Fractal characteristics and growth stage division of shrub root system parameters

The application of a fractal statistical model enabled the classification of distinct growth stages within the *Kalidium* shrub's root system, based on unique fractal dimensions (D). This approach laid the groundwork for categorizing the stages.

In this study, logarithmic transformations were applied to the root length and diameter of 234 shrub samples, which were then plotted on $Lgr-LgN(r)$ coordinates (Fig. 6). The least squares method was used to derive the corresponding linear equations, fractal dimensions, and threshold points (Table 5). All equations had R-squared values (R^2) above 0.8, confirming their statistical significance.

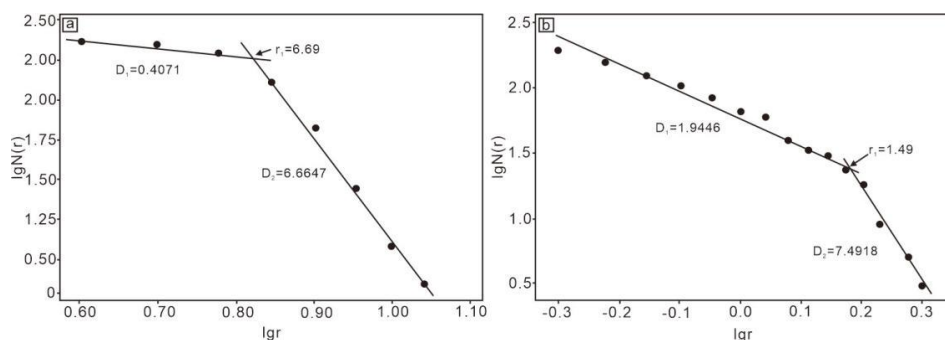


Figure 6. (a) Distribution of root length $lgN-lgr$ of *Kalidium*. (b) Distribution of ground diameter $lgN-lgr$ of *Kalidium*

Table 5. Fitting results of fractal model of root length and ground diameter of *Kalidium*

Morphological parameters	Fractal model	R^2	Fractal dimension	Fitting range
Root length	$\ln N = -0.4071 \ln r + 2.6175$	0.8789	0.4071	$r \leq 6.69$
	$\ln N = -6.6647 \ln r + 7.7835$	0.9345	6.6647	$r > 6.69$
Root diameter	$\ln N = -1.9446 \ln r + 1.7790$	0.9756	1.9446	$r \leq 1.49$
	$\ln N = -7.4918 \ln r + 2.7462$	0.9773	7.4918	$r > 1.49$

The fractal distribution characteristics of the root system parameters of *Haloxylon ammodendron* allow for the determination of extreme values using fractal statistical models (Wang and Wang, 2007). Equation 1 suggests that when $N(r) = 1$, indicating that the cumulative number of clusters with root system parameters greater than r is 1, then $r = C^{1/D}$ represents the extreme value. Calculations revealed that the maximum root length (R_{max}) is 14.72 cm and the maximum ground diameter (GD_{max}) is 2.33 cm.

By integrating the fitting intervals and extreme values of root length and ground diameter using the fractal statistical model, the 234 samples of *Haloxylon ammodendron* shrub roots were classified into three distinct growth stages: Growth Stage (I), Mature Stage (II), and Senescence Stage (III) (Table 6).

Figure 7 illustrates the Cartesian projection of root length and ground diameter for the 234 samples. By applying the stage divisions from Table 6, it is possible to effectively categorize the samples and distinguish between the various growth stages of *Kalidium* shrub roots.

Table 6. Criteria for different growth stages of root system of kalidiums

Growth stage	Growth period (I)	Mature period (II)	Senescence period (III)
Root length / cm	0-6.69	6.69-14.72	14.72-0
Ground diameter / cm	0-1.49	1.49-2.33	2.33-0

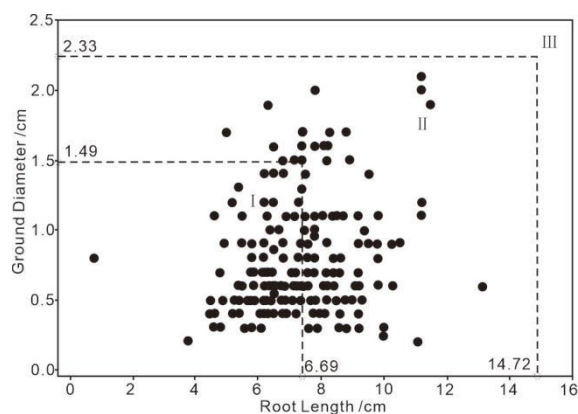


Figure 7. Division of root growth stages of kalidiums

***Kalidium* shrubs growth process**

Relationship between horizontal expansion and upright growth of kalidium shrubs canopy

Adopting a semi-ellipsoidal shape for the above-ground canopy structure of *Kalidium* shrubs, we can approximate the canopy area (CA) as an ellipsoid. The formula for calculating the canopy area (CA) is given by Equation 11:

$$CA = \pi ab / 4 \quad (\text{Eq.11})$$

The differential form of the Malthusian growth model suggests that the relative growth rate of individual organisms or parts is directly proportional to the growth time, as indicated by Xu (2004). This principle leads to Equation 12, which describes the

vertical growth (stem elongation) and horizontal expansion (canopy radius enlargement) of shrub canopies:

$$CA = C^* \times H^{2\gamma} \quad (\text{Eq.12})$$

By taking the logarithm of both sides of the equation, we derive *Equation 13*:

$$\lg CA = 2\gamma \lg H + \lg C^* \quad (\text{Eq.13})$$

Through linear regression on $\lg CA - \lg H$, we determine the parameter γ , which represents the ratio of the growth rate of canopy radius to the growth rate of stem height in the shrub. Subsequent variance analysis and an F-test, with $p < 0.05$, confirm the statistical significance of our linear regression model and validate its goodness-of-fit based on the determination coefficient (R^2).

When we take the first and second derivatives of *Equation 12* with respect to H , we arrive at *Equations 14* and *15*, respectively.

$$\frac{dCA}{dH} = 2\gamma C^* H^{2\gamma-1} \quad (\text{Eq.14})$$

$$\frac{d^2CA}{dH^2} = 4\gamma(\gamma-1)C^* H^{2(\gamma-1)} \quad (\text{Eq.15})$$

It becomes clear that the derivative is always positive, signifying that both the first and second derivatives are functions that increase monotonically. Nevertheless, let us delve deeper into the implications of the second derivative under various conditions:

In the case where $\gamma > 1$, the equation characterizes a concave function. This suggests that as the stem height increases, the relative growth rate of the crown width will eventually exceed that of the stem height. Consequently, this leads to a preferential expansion of the crown in a more horizontally flattened direction.

Conversely, when $\gamma < 1$, the equation takes on a convex form. This indicates that with the growth in stem height, the relative growth rate of the stem itself will gradually outpace that of the crown radius. As a result, the crown is inclined to expand predominantly in a vertical direction.

When γ fluctuates around the value of 1, the equation oscillates between concavity and convexity. This transition implies that the relative growth rates of the crown width and stem height maintain a state of equilibrium as the stem height extends. Consequently, this balanced growth leads to the crown adopting an approximately hemispherical configuration.

Simulation of different growth stages of kalidium shrubs canopy

We classified the shrub canopy of *Kalidium* based on the stages depicted in *Figure 7*. Logarithmic scatter plots and linear regression analyses were conducted for canopy width and branch height, considering the entire dataset as well as each growth stage (*Fig. 8*). The variance analysis and F-test results, with $p < 0.05$, affirm the statistical significance of *Equation 13*. However, the relatively low determination coefficients suggest variability among different stages of the shrubs.

The regression results indicate that the overall γ for the *Kalidium* shrub canopy is 1.2, suggesting a generally balanced relative growth rate between canopy width and branch height across the entire growth stage, leading to a development towards a semi-spherical canopy shape. In the juvenile stage, γ exceeds 1.5, indicating that the relative growth rate of canopy width surpasses that of plant height, leading to a flatter canopy shape. In contrast, during the growth stage, γ drops below 0.3, signifying that the relative growth rate of branch height surpasses that of canopy width, resulting in a more vertical canopy shape. In the maturity stage, γ equals approximately 0.8, implying a slight variation from unity or balance between relative rates, leading to further progression towards semi-spherical canopies.

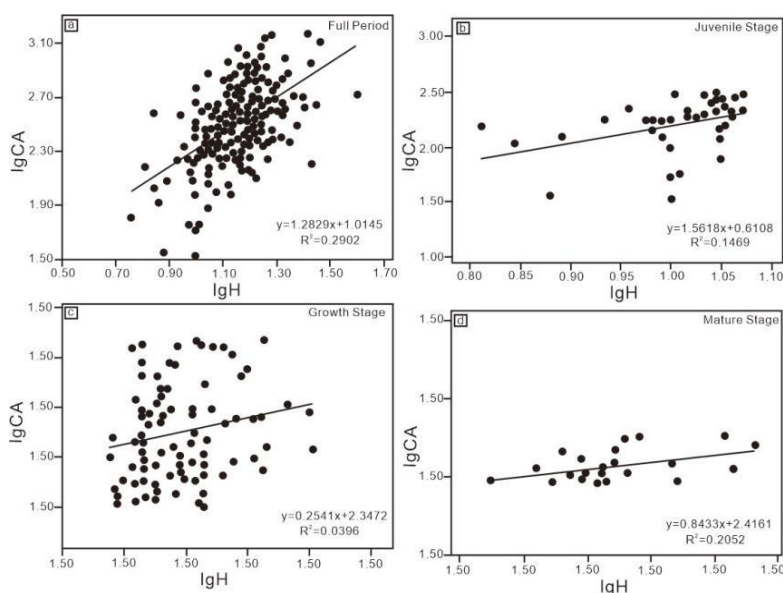


Figure 8. The lgH - $lgCA$ map of different stages of the canopy of *kalidiums*

Based on the aforementioned findings, a model simulating the growth scenario of the *Kalidiums* shrub canopy has been developed (Fig. 9). The model's growth curves delineate three distinct developmental stages: an initial phase marked by slow expansion, predominantly in canopy width, during the shrub's juvenile period. This is succeeded by a phase of rapid growth, primarily in terms of branch height. The final stage sees a return to a slower growth rate, with a focus on increasing canopy width, as the shrub matures. This model effectively encapsulates the dynamic trends in the growth and development of the shrub canopy.

By categorizing the stages of shrub canopy development into three distinct forms—flat, vertical, and semi-spherical—it becomes clear that each stage presents a unique shape. As illustrated in Figure 9, during the juvenile phase of the *Kalidiums* shrub, when the branch height is relatively low, the canopy exhibits a flat profile. In the subsequent growth phase, there is a significant increase in branch height until it reaches its maximum potential, while the growth rate for canopy width changes minimally, maintaining the flat-shaped appearance. In the mature stage, both horizontal expansion and vertical growth are moderated within the shrub's canopy. Of particular interest is the early attainment of the maximum branch height, which leads to a gradual transition towards a semi-spherical canopy shape.

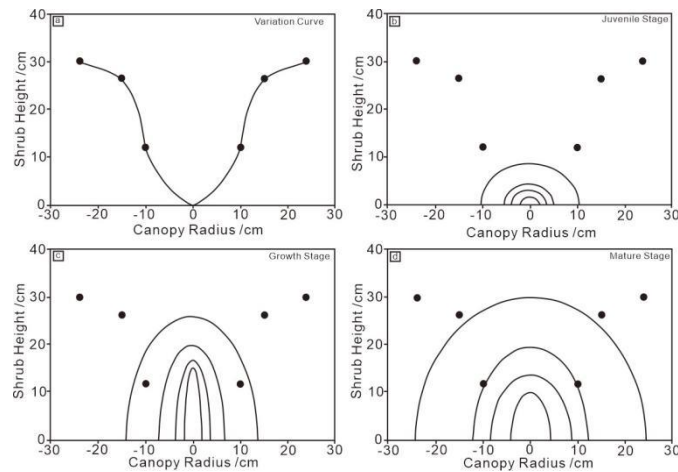


Figure 9. Canopy growth and evolution of kalidiums shrub

Relationship between the thickening of shrub roots and stems and downward growth of roots

Assuming the underground root structure of the *Salix cheilophila* shrub takes a conical shape, the cross-sectional area of the underground root structure (*GDA*) can be considered as a circular surface. The calculation for determining the *GDA* is described by Equation 16:

$$GDA = \pi GD^2 \tag{Eq.16}$$

The relationship between the downward growth of shrub roots (root elongation) and the expansion of root stems (increase in ground diameter radius) is derived as Equation 17:

$$R = C^* \times GD^\gamma \tag{Eq.17}$$

Where C^* is a constant, and γ represents the ratio of shrub root growth rate to ground diameter growth rate. Taking the logarithm of both sides of the equation yields Equation 18:

$$\lg R = \gamma \lg GD + \lg C^* \tag{Eq.18}$$

By performing a linear regression analysis on $\lg R - \log GD$, we obtain the parameter γ . The first and second derivatives of R with respect to GD yield Equations 19 and 20, which help us understand the growth dynamics under different γ values.

$$\frac{dR}{dGD} = \gamma C^* GD^{\gamma-1} \tag{Eq.19}$$

$$\frac{d^2R}{dGD^2} = \gamma(\gamma-1)C^* GD^{\gamma-2} \tag{Eq.20}$$

The function's nature, as described by the variable γ , consistently maintains a positive value, denoted by $\gamma > 0$. This positivity, coupled with the first derivative also

being positive, $\gamma' > 0$, confirms that the function is monotonically increasing. This characteristic suggests a continuous growth pattern without any diminishing returns.

Delving deeper into the function's curvature, the second derivative offers a nuanced perspective on how the growth rates of the shrubbery's root diameter and length interact:

When $\gamma > 1$, the function exhibits concavity. This geometric property implies that the growth rate of the shrubbery's root diameter becomes increasingly more significant relative to the growth rate of its root length as the length expands. Consequently, this leads to a more pronounced horizontal development of the root system, with a focus on expanding the diameter and surface area of the roots.

Conversely, if $\gamma < 1$, the function is convex. In this scenario, the relative growth rate of the root length begins to overshadow that of the root diameter as the diameter increases. This suggests a vertical emphasis in the root system's development, with the roots growing deeper into the soil to access nutrients and water.

When γ fluctuates around the value of 1, the function's curvature transitions between convex and concave. This transition indicates a dynamic equilibrium between the relative growth rates of root length and diameter. As such, the root system is inclined to evolve into a shape that approximates a conical form, balancing both horizontal and vertical growth to optimize resource acquisition.

Simulation of different growth stages of shrubbery root systems

The root systems of *Kalidiums* shrubbery were meticulously extracted and classified according to the developmental stages depicted in *Figure 7*. We conducted scatter plot analyses on double logarithmic scales and performed linear regression for the overall and individual growth stages of both root length and diameter, as illustrated in *Figure 10*. The variance analysis and F-test results revealed statistical significance ($p < 0.05$) across all stages of the shrubbery, corroborating *Equation 18*. However, the determination coefficients were relatively modest, highlighting the variability among the different growth stages.

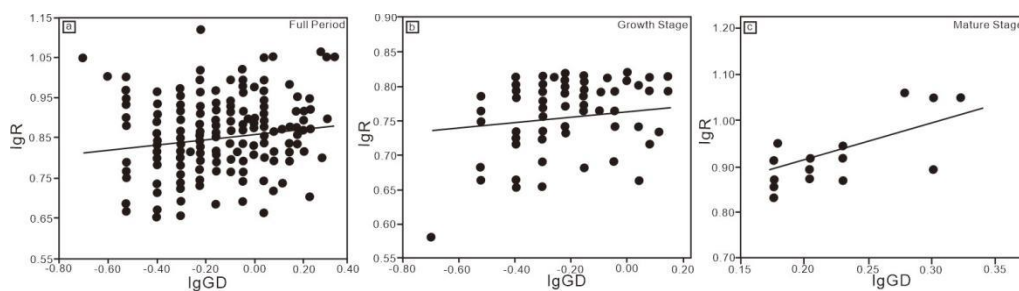


Figure 10. LgGD-LgR diagrams for various growth stages of the root system of *kalidium*s

From the regression findings, it was observed that $\gamma = 0.0668$ for the entire root system of the salt claw shrubbery, which is less than 1. This suggests that the relative growth rate of root length is significantly higher than that of root diameter, indicating a pronounced vertical growth pattern throughout the plant's development. During the growth phase, γ stood at 0.0378, also less than 1, signifying a gradual shift in the relative growth rate in favor of length over diameter as the plant size increases, maintaining a vertical growth pattern. In the mature phase, γ rose to 1.0922, indicating a

near equilibrium between the relative growth rates of both parameters, leading to the development of a nearly conical form.

Drawing from these results, we simulated a growth scenario model for the salt claw shrubbery canopy (Fig. 11). Upon scrutinizing the growth curve of the shrubbery root system, it became clear that the system initially experiences rapid growth, primarily driven by root length, before transitioning to a phase of balanced growth between diameter and length. This pattern effectively mirrors the actual growth behavior of plant root systems. By classifying the growth stages based on longitudinal cross-sections, two distinct types of root systems were identified: near-cylindrical and near-conical. The varied root systems exhibited at different growth stages of the shrubbery are depicted in Figure 11. Initially, there is a slow increase in root diameter, leading to a near-cylindrical shape. As maturity is reached, rapid elongation occurs until it plateaus with a significantly slower relative rate of length increment. Both vertical and horizontal expansion are constrained in the mature stage, particularly for length extension, which is limited early on, leading to a transition towards a near-conical shape. In this section, correlation analysis was employed to pinpoint model parameters closely linked to biomass.

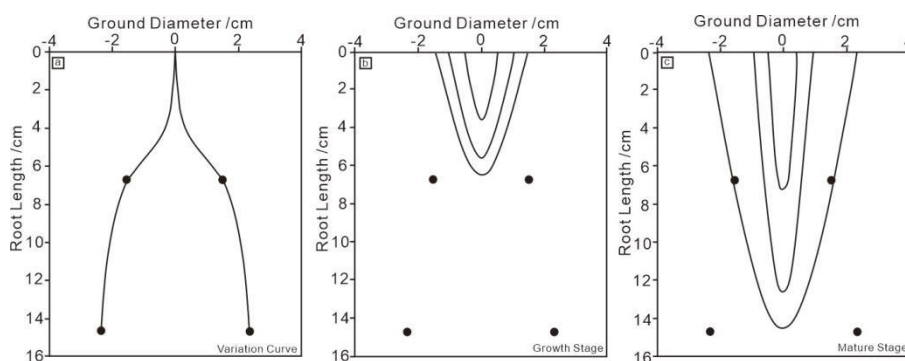


Figure 11. Root system growth and evolution diagram of *Kalidium*s

***Kalidium*s shrub biomass model**

Biomass is a key indicator of an ecosystem's energy acquisition capacity and significantly influences the formation of ecosystem structure (Yu and Yu, 2001). Historically, research on biomass has focused on arboreal components in cultivated lands, grasslands, and forest vegetation (Lu and Gong, 2009). In contrast, shrubbery forests have received less attention due to their smaller proportion and fewer reports on their biomass (Zeng, 2015). The distinctive morphology and community structure of shrubs result in a biomass profile that differs from trees and herbaceous plants. Directly predicting individual biomass using binary tree volume equations for trees is challenging, and the discontinuities and non-uniformity in horizontal distribution of shrubs make them unsuitable for biomass determination using plot-based harvesting methods more applicable to herbaceous plants (Liu, 1994).

Common methods for shrub biomass determination include the plot method, average tree method, quantitative method, and allometric method. The plot method can provide relatively precise biomass data (Feng and Wang, 1999), but its labor-intensive nature makes it impractical for shrub biomass assessment. The average tree method, while straightforward, has been critiqued for potentially failing to represent an average tree

across different dendrometric indices (Oington et al., 1963; Attiwill, 1966; Baskerville, 1965). The quantitative method, which involves quantifying various factors affecting biomass and integrating both quantitative and qualitative indicators, yields more accurate results but is hindered by complex model structures (Jiang et al., 1997). The allometric method, widely accepted in ecological literature for estimating shrub biomass, offers a labor-efficient solution with minimal ecological impact (Feng and Wang, 1999). Recent research has focused on developing theoretical models based on physiological processes and fractal geometry to integrate allometric growth patterns across diverse biological realms (West et al., Brown, 1999; Enquist and Niklas, 2002).

In this study, we utilized theoretically derived allometric fractal equations to construct separate above-ground and below-ground biomass models for desert salt claw shrubbery. This work provides a vital reference for biomass modeling in other shrubby vegetation within the Heihe River Basin, contributing to the advancement of our understanding in this field.

Selection of biomass model parameters

The prerequisite for constructing a biomass prediction model is a significant correlation between the independent variables and various components of biomass (Wu et al., 2012). Increasing the number of independent variables can often lead to more accurate biomass estimates in statistics (Saint-André et al., 2005; Wang, 2006), although this is not always the case (Ter-Mikaelian and Korzukhin, 1997). We selected variables such as shrub height (H), ground diameter section (GDA), root length (R), root-to-height ratio (R/H), aboveground biomass (W_A), and belowground biomass (W_S) for correlation analysis.

Table 7 reveals that aboveground biomass (W_A) exhibits highly significant correlations with shrub height (H), canopy radius (C), canopy area (CA), and canopy volume (V), with shrub height (H) and canopy area (CA) showing the highest correlation coefficients. Belowground biomass (W_S) shows highly significant correlations with ground diameter section (GDA) and root length (R), with GDA having the highest correlation coefficient.

Therefore, it is advisable to construct above-ground biomass (W_A) models using canopy morphological parameters such as shrub height (H) and canopy area (CA). Similarly, below-ground biomass (W_S) models should employ root system morphological parameters like ground diameter section (GDA) and root length (R).

Table 7. Correlation coefficient matrix between parameters and biomass of *kalidiums*

Variable	H	C	CA	V	GDA	R	R/H	W_A	W_S
H	1								
C	0.478**	1							
CA	0.452**	0.975**	1						
V	0.672**	0.884**	0.929**	1					
GDA	0.373**	0.528**	0.507**	0.518**	1				
R	0.128*	0.217**	0.236**	0.225**	0.174**	1			
R/H	-0.686**	-0.311**	-0.255**	-0.379**	-0.207**	-0.522**	1		
W_A	0.891**	0.752**	0.873**	0.778**	0.225**	0.223**	-0.282	1	
W_S	0.3**	0.522**	0.538**	0.552**	0.806**	0.871**	-0.044	0.64**	1

* indicates significant correlation at the 0.05 level; ** indicates highly significant correlation at the 0.01 level

Establishment of biomass models

Utilizing the allometric growth fractal theory and selected morphological parameters derived from correlation analysis, a model was developed based on measured data to estimate the above-ground biomass of the *kalidiums* shrubbery. After applying logarithmic transformations to the variables, a scatter plot was created (Fig. 12a). Subsequently, a fractal relationship between the biomass and the crown morphological parameters of the salt claw shrubbery was precisely fitted (Fig. 12b). In the scatter plot, the above-ground biomass (W_A) demonstrates a linear planar trend in relation to both the shrub height (H) and the canopy area (CA). Based on this linear relationship, a planar equation was derived through linear planar fitting:

$$\text{Lg}W_A = 0.3777 \times \text{lg}H + 0.0035 \times \text{lg}CA - 0.3850 \quad R^2 = 0.9889$$

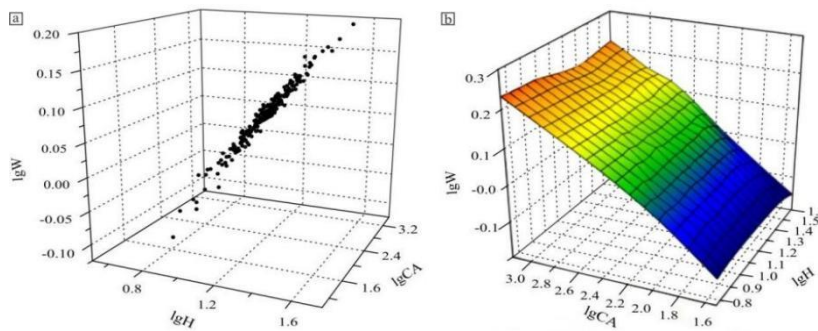


Figure 12. Scatter plots (a) and logarithmic plane fitting plots (b) of the branch height-crown width-above-ground biomass of *kalidiums*

The below ground biomass (W_S) model underwent a similar process of data transformation, scatter plot projection, and planar fitting, as depicted in Figure 13a, b. The resulting planar equation is presented below:

$$\text{lg}W_S = 0.9073 \times \text{lg}R + 0.9113 \times \text{lg}GDA - 0.2013 \quad R^2 = 0.839$$

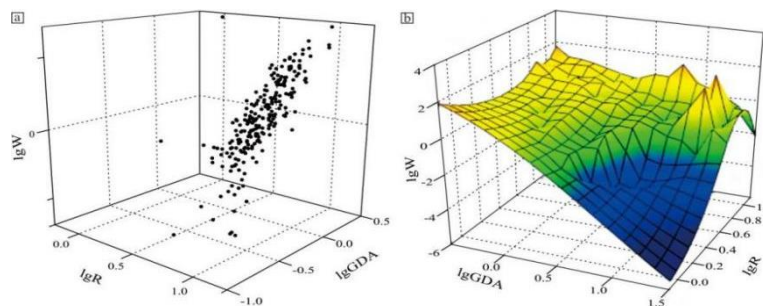


Figure 13. Scatter plots (a) and logarithmic plane fitting plots (b) of cross-section-root length-underground biomass of *kalidiums*

When it comes to model selection, the determination coefficient (R^2) should ideally be high, the Standard Error of the Estimate (SEE) should be minimal, and the

regression relationship must be statistically significant, as confirmed by passing the F-test. In the case of the above-ground biomass (W_A) model for salt claw shrubbery, which utilizes shrub height (H) and canopy area (CA) as morphological parameters, the R^2 value was remarkably high at 0.9889, accompanied by an exceedingly low SEE of 0.0053. Moreover, the F-value of 10344.6722 robustly passed the significance test.

For the below-ground biomass (W_S) model, which incorporates ground diameter (GD) and root length (R) as morphological parameters for salt claw shrubbery, a high R^2 value of 0.839 was achieved, with a moderate SEE of 13.7549. The F-value also successfully passed the significance test with a score of 331.4949.

It is important to note, however, that in comparison to above-ground biomass estimation models (W_A), below ground biomass estimation models (W_S) tend to have smaller R^2 values. This difference may be ascribed to potential shortcomings in sampling complete root systems from salt claw shrubbery samples or to inaccuracies in measuring root system morphological parameters, both of which could contribute to a reduced model fit.

In summary, the application of allometric growth fractal theory in conjunction with morphological parameters has proven to be a powerful tool in the development of biomass models. The high R^2 values and low SEE values indicate a strong predictive capacity for both above-ground and below-ground biomass estimation. Despite the challenges associated with below-ground biomass estimation, the models developed provide a solid foundation for further research and refinement in the field of biomass modeling.

Conclusion

(1) This study used fractal statistical models to classify different growth stages of salt claw shrubbery based on the investigation of morphological parameters in the crown and root system. The crown growth stages were identified as flat-vertical-nearly hemispherical, while the root system growth stages were identified as vertical-horizontal-nearly cone-shaped. The results demonstrate that shrubs can exhibit a development trend characterized by flat, nearly hemispherical, and vertical forms, with height limitations imposed by the vascular water transportation system leading to a rapid attainment of their maximum growth potential during adulthood.

(2) By combining biological growth stages and deducing a fractal model from a theoretical perspective, this paper elucidates the relationship between biological morphology and biomass, presenting a universal rule that can be widely applied.

(3) The generalized allometric fractal model of biomass developed in this study effectively correlates the above-ground biomass of individual shrubs with easily measurable morphological parameters, enabling non-destructive, time-sensitive, and accurate biomass observation.

Acknowledgements. This work was financially supported by the “Investigation, monitoring and evaluation of water conservation and ecological degradation in plateau mountains of Heihe River basin and Geological survey of regional ecological protection and restoration in the lower reaches of Heihe River” (DD20220883, DD20242544, DD20243409).

Conflict of interest. The authors declare no competing interests.

REFERENCES

- [1] Attiwill, P. M. (1966): A method for estimating crown weight in eucalyptus, and some implications of relationships between crown weight and stem diameter. – *Ecology* 47(5): 795-804.
- [2] Baskerville, G. L. (1965): Estimation of dry weight of tree components and total standing crop in conifer stands. – *Ecology* 46(6): 867-869.
- [3] Cai, T. J., Ju, C. Y., Yang, X. H. (2009): Comparison of ridge regression and partial least squares regression for estimating above-ground biomass with Landsat images and terrain data in Mu Us sandy land, China. – *Arid Land Research and Management* 23(3): 248-261.
- [4] Chang, J., Chen, G., Ge, Y. (1996): A new method for quantitative study of plant morphology and structure-fractal simulation. – *Botanical Bulletin* 13(2): 57-62.
- [5] Chang, X. L., Wu, J. G. (1996): Application of fractal model in ecological research. – *Journal of Ecology* 15(3): 35-42.
- [6] Dong, L. P., Hu, X. J., Yang, W. L. (2024): Study on crown prediction model of *Haloxylon ammodendron* in different habitats. – *Forest Engineering* 40(4): 1-10.
- [7] Enquist, B. J., Niklas, K. J. (2002): Global allocation rules for patterns of biomass partitioning in seed plants. – *Science* 295: 1517-1520.
- [8] Enquist, B. J., West, G. B., Charnov, F. L., Geoffrey, B. (1999): Allometric scaling of production and life-history variation in vascular plants. – *Nature* 401(6756): 907.
- [9] Feng, Z. W., Wang, X. K. (1999): *Biomass and Productivity of Forest Ecosystems in China*. – Science Press, Beijing.
- [10] Gao, J., Zhang, J. S., Meng, P. (2004): Fractal theory and its application in forestry science. – *World Forestry Research* 17 (6): 11-16.
- [11] Houghton, R. A., Hall, F., Goetz, S. J. (2009): Importance of biomass in the global carbon cycle. – *Journal of Geophysical Research* 114: G00E03.
- [12] Huang, J. S., Di, X. Y. (2011): Estimation model of above ground biomass of 6 shrubs in Maershan area. – *Journal of Northeast Forestry University* 39(5): 54-57.
- [13] Jiang, J., Liu, G. B., Liang, Y. M. (1997): A non-destructive measuring plate for shrub biomass. – *Notification of Soil and Water Conservation* 17(1): 43-46.
- [14] Li, L., Zhou, D. W., Sheng, L. X. (2011): The distribution pattern of plant biomass determined by density. – *Journal of Ecology* 30(8): 1579-1589.
- [15] Li, X. L., Ling, H. L. (2011): Application of fractal theory in grassland science. – *Journal of Grassland Science* 19(4): 706-711.
- [16] Liu, C. Q. (1994): Studies on techniques for determining shrub biomass. – *Journal of Prataculture* 3(4): 61-65.
- [17] Lortie, C. J., Turkington, R. (2002): The effect of initial seed density on the structure of a desert annual plant community. – *Journal of Ecology* 90(3): 435-445.
- [18] Lu, Z. L., Gong, X. S. A. (2009): Advances in the measurement of shrub biomass. – *Forestry Survey Planning* 34(4): 37-41.
- [19] Mandelbrot, B. B. (1982): *The Fractal Geometry of Nature*. – W H Freeman, New York.
- [20] McConnaughay, K. D. M., Coleman, J. S. (1999): Biomass allocation in plants: ontogeny or optimality? A test along three resource gradients. – *Ecology* 80(8): 2581-2593.
- [21] Niklas, K. J. (2004): Modelling below-end above-ground biomass for non-woody end woody plants. – *Annals of Botany* 95(2): 315-321.
- [22] Oington, J. D., Dale, H., Donald, B. (1963): Plant biomass and productivity of prairie, savanna, oak-wood, and maize field ecosystems in Central Minnesota. – *Ecology* 44(1): 52-63.
- [23] Ren, J. Z. (2008): *Dictionary of Grass Industry*. – China Agricultural Press, Beijing, pp. 202-203.
- [24] Saint-André, L., M'Bou, A. T., Mabiala, A., Mouvondy, W., Jourdan, C., Roupsard, O., Deleporte, P., Hamel, O., Nouvellonet, Y. (2005): Age-related equations for above-and below-ground biomass of a *Eucalyptus* hybrid in Congo. – *For EcolManag* 205: 199-214.

- [25] Shen, W., Zhao, P. D. (1998): Theoretical study of fractal statistical model and its application in geology. – *Forestry Survey Planning* 33(2): 234-242.
- [26] Tao, Y., Zhang, W. M. (2013): Multi-scale estimation of desert shrub biomass-a case study of *Haloxylon ammodendron*. – *Journal of Grass Industry* 22(6): 1-10.
- [27] Ter-Mikaelian, M. T., Korzukhin, M. D. (1997): Biomass equations for sixty-five North American tree species. – *For Ecol Manag* 97: 1-24.
- [28] Wang, C. (2006): Biomass allometric equations for 10 co-occurring tree species in Chinese temperate forests. – *For Ecol Manag* 222: 9-16.
- [29] Wang, J., He, B. Y. (2017): Study on understory shrub biomass growth model in Altai mountains. – *Anhui Agricultural Science* 45(36): 157-160.
- [30] Wang, J. F., Ou, G. L., Tang, J. R., Lu, Z. L., Li, H. L., Xu, H. (2012): Study on biomass estimation model of shrub community in *Jatropha curcas* plantation area in Lincang. – *Western Forestry Science* 41(6): 53-58.
- [31] Wang, L., Wang, Q. F. (2007): Limit resource model and application. – *Geological Science and Technology Information* 26(4): 8-10.
- [32] West, G. B., Brown, J. H., Enquist, B. J. (1999): A general model for the structure and allometry of plant vascular systems. – *Nature* 400: 664-667.
- [33] Wu, X. D., Xie, Y. Z., Xu, K., Wang, S. P., Zhang, X. J. (2012): Biomass allocation and estimation models of wine grape plantations with different plant ages in the eastern foothills of Helan Mountains. – *Chinese Journal of Ecological Agriculture* 20(10): 1322-1328.
- [34] Xu, K. F. (2004): *Mathematical and Theoretical Biology*. – Science Press, Beijing, pp. 214-220.
- [35] Yu, W. T., Yu, Y. Q. (2001): Advances in the study of plant underground biomass. – *Journal of Applied Ecology* 12(6): 927-932.
- [36] Zeng, W. S. (2015): A review of studies on shrub biomass models at home and abroad. – *World Forestry Research* 28(1): 31-36.
- [37] Zhang, C., Wang, L. D., Geng, S. B., Lu, S. (2012): A review on the application of box-counting dimension in population spatial distribution pattern. – *Forestry Survey Planning* 37(5): 47-50.
- [38] Zhang, Z. Y., Zhao, X., Li, G. (2016): Distribution characteristics of biomass and carbon and nitrogen contents in different organs of 6 shrubs. – *Grasslands and Lawns* 36(3): 23-27.
- [39] Zhao, K. F., Fan, H., Jiang, X. Y., Song, J. (2002): The role of halophytes in the improvement of saline soils. – *Journal of Applied and Environmental Biology* 8(1): 31-35.
- [40] Zheng, S., Shang, G. Z. (2004): Stomata-density changes of the plants in the Loess Plateau of China over last century. – *Acta Ecologica Sinica* 24: 2457-2464.
- [41] Zheng, S. W., Tang, M., Zou, J. H., Mu, C. L. (2007): Review of studies on shrub community and biomass. – *Journal of Chengdu University (Natural Science Edition)* 26(3): 189-192.